COBEM 2021 26th International Congress of Mechanical Engineering
November 22-26, 2021, Virtual Congress, Brazil

COB-2023-0625 INFLUENCE OF HEATING A PORT FUEL INJECTION SYSTEM ON HYDROUS ETHANOL IN AN OPTICALLY ACCESSIBLE SPARK IGNITION ENGINE

Frederico Weissinger
AVL South America - frederico.weissinger@avl.com
Pedro Lacava
Alexander Penaranda
Andre Martelli
Fábio Dias
Enrico Rapetti Malheiro de Oliveira
Leila Ribeiro dos Santos
Laboratório de Combustão, Propulsão e Energia, Instituto Tecnológico de Aeronáutica, São José dos Campos, São Paulo
Vincent Bigliardi
AVL South America

Abstract. *The increase in energy demand due to population growth and the rise in living standards is a well-established trend. Such demand for energy cannot be met solely by fossil fuels, given the associated adverse effects such as pollution, climate change, and natural disasters. Furthermore, stricter CO2 emission regulations require advanced engine technologies to comply with the progressive limits. Consequently, there has been an upsurge in interest in synthetic and renewable fuels (such as ethanol) in spark ignition engines aiming at mitigating CO2 emissions and reducing greenhouse impacts. However, to limit unburned hydrocarbons and other emissions during the cold start phase, ethanol heating devices are required in MPI systems. In this context, this research used an optical single cylinder to study the early cold phase of a spark ignition engine with a heated multi-hole port fuel injector using hydrous ethanol (containing 5% water). A fuel temperature of 10°C and three injector tip temperatures were compared at both 1200 and 2000 rpm and stoichiometric air-fuel ratio. Optical measurements were taken using a quartz piston window and a quartz cylinder liner, and from each flame propagation and fuel film formation analyses were performed. The optical measurements were also compared with the thermodynamic parameters derived from cylinder pressure measurements. The results indicate higher fuel vaporization, flame propagation speed, and indicated mean effective pressure when the injector was heated, especially at 1200 rpm, where the late ignition strategy for catalyst heat up (spark at TDC) induces greater instabilities.*

Keywords: *Ethanol, heated injector, PL8, combustion engine,*

1. INTRODUCTION

As ethanol has a characteristic of its flash point at 12°C that makes cold starts below this threshold difficult or even not impossible, the earliest ethanol-fueled vehicles had a secondary fuel system responsible for delivering gasoline to the engine in cold starts, which is not possible to be used anymore due to the restrictions in tail-pipe emissions legislation and in evaporative emissions. The solution was implementing a device that was capable of rapidly electrically heating the ethanol fuel via fuel injector technology. These heated fuel injectors can be used for cold-starting ethanol-fueled engines and to enable emissions reduction with a variety of automotive fuels after PROCONVE Level 6. Additionally, it made it possible to comply with current strict restrictions that require Brazilian legislation to take unburned ethanol (ETOH) pollution into account. These benefits also enable the reduction of fuel consumption with E100 and potential catalytic converter savings through significant fuel injection optimization on cold start and emissions. When it is focused on the next generation of emissions legislation, it must be mentioned the PROCONVE Level 8, which the main challenge is related to NMOG (Non-Methane Organic Gases), which besides NMHC also includes the organic gases ethanol and aldehydes. During the cold phase especially using pure Ethanol, the emission of NMOG normally is higher than E22, which requires a system in order to reduce the emissions of this specific gas. For that reason, it was selected for this study device mentioned previously normally used in flex-fuel vehicles with a PFI system that is capable of heating the fuel in the injector in a very short time, nevertheless with new technology to improve the fuel heat-up phase. This study will be focused on the assessment of the propagation of the ethanol flame in an engine with optical access, with the preparation of the mixture based on a PFI injection system with heating. For execution, a research engine bench with optical access located at the Laboratory of Combustion, Propulsion, and Energy (LCPE) of ITA in the city of São José dos Campos, SP was used.

2. EXPERIMENTAL METHODOLOGY

2.1 CONFIGURATION OF SINGLE CYLINDER ENGINE BENCH

The experiments were conducted on a single-cylinder research engine bench with AVL 5405 optical access, which has the following features:

Diameter [mm]	82	Intake valve diameter [mm]	34
Stroke [mm]	90	Exhaust valve diameter [mm]	26
Displacement [cm3]	475	Intake valve opening [CAD]	345
Compression ratio	9.64:1	Intake valve closing [CAD]	-140
Number of intake valves	2	Exhaust valve opening [CAD]	123
Number of exhaust valves	2	Exhaust valve closure [CAD]	-337

Table 1 – Optical engine characteristics

The in-cylinder pressure data were acquired by an AVL GU22C piezoelectric pressure transducer and an IndiModul 622 acquisition system. The crankshaft angle was measured by an AVL 365C encoder. The pressure of the intake and exhaust manifolds was measured by two AVL LP11DA pressure transducers. Air and fuel flow rates were measured by an AVL Flowsonix AT4456E ultrasonic mass flow meter and an AVL Fuel Balance AT0905E, respectively. In order to analyze the heat release curve, the AVL Indicom software was used, taking the pressure curve inside the cylinder as a reference. The air-fuel ratio was measured by a Bosch LSU 4.9 lambda sensor and the signal was conditioned by an ETAS ES636.1 module. The ignition and injection times and the synchronization of the high-speed camera used to obtain images of the flames were defined using an AVL 427 Engine Timing Unit (ETU) control unit. The piston is equipped with a quartz window, which allows the natural luminosity of the flame to reflect in a mirror mounted at 45°, directing the luminosity toward the camera.

The combustion was maintained in conditions close to stoichiometric, with ignition advance set to maximum torque (maximum indicated mean effective pressure -IMEP) at 2000 rpm. The injection time was adjusted to provide a load of 4.86 bar of IMEP in the reference condition, fuel at 20°C and without injector heating. Each test lasted about 250 engine cycles. Thermodynamic data were calculated from the last 100 cycles, while the last 30 engine cycles were used for optical flame propagation analysis.

Additionally, operations at 1200 RPM were studied in order to characterize combustion during the warm-up phase of the engine and gas after-treatment systems, with delayed ignition occurring at the top dead center. In this case, the injection time was adjusted to promote 4.10 bar IMEP in the reference condition. The fuel temperature was controlled using the AVL 753C-600 system, with two operating conditions defined: 10°C and 20°C. The coolant and lubricant were not heated by the conditioning systems, remaining close to ambient temperature.

The ambient temperature (test cell) was reduced to the lowest possible by the air conditioning system, stabilized at 17°C throughout the tests, from which the intake air was captured. The injection nozzle heating temperature was controlled through the ETAS INCA software using the Multec 3.5HT Gen 2 system supplied by the Borg Warner company. Tests were carried out under three nozzle heating conditions: without heating (room temperature), 100 °C and 150°C. The engine operating conditions are shown below in Table 2.

TEST	SPEED	T_fuel	T_injector	T_cylhead	T_amb	T_air	SOI	DOI	Spark timing
	[rpm]	[°C]	[°C]	[°C]	[°C]	[°C]	[°CA]	[ms]	[°CA]
1.1	1200	10	amb	30	17	20	285	19	0
1.2	1200	20	amb	30	17	20	285	19	0
1.3	1200	10	175	30	17	20	285	19	0
1.4	1200	20	175	30	17	20	285	19	0
2.1	2000	20	amb	30	17	19	285	18	-8
2.2	2000	10	amb	30	17	19	285	18	-8
2.3	2000	20	175	31	17	20	285	18	-8
2.4	2000	10	175	31	17	20	285	18	-8

Table 2 - Engine operating conditions for each test performed.

2.2 INJECTION SYSTEM DESCRIPTION

The Multec 3.5HT Gen 2 system supplied by Borg Warner company, incorporates a heating element at the base of the injector to the traditional PFI fuel injection system. This aims to reduce the fuel heating time and improve its evaporation in critical phases, as in cold start. Such a device is especially useful for engines operating with ethanol since due to the absence of volatile fractions in the fuel (abundant in gasoline), the preparation of the mixture is deficient in the low temperatures of the cold start. The system employs high starting electric currents and closed-loop temperature control of the heating resistor at the base of the injector, in order to maximize heat transfer to the fuel in the region immediately before the fuel flow control valve, allowing vaporization of the liquid even at low temperatures (Ambient temperatures around -5°C). In addition to improving engine starting, the Multec 3.5HT warm-up function also aims to reduce unburned fuel emissions during the warm-up phase. In this way, the system aims to overcome critical deficiencies in the efficiency and performance of internal combustion engines that use ethanol as fuel, in the period that comprises the first cycles of operation.

2.3 IMAGE ACQUISITION AND PROCESSING SYSTEM

Figure 1 shows the experimental arrangement for viewing the flame and fuel spray in the optical access engine. The visualization of the combustion process for the study of flame propagation was performed through the chemiluminescence of the species produced by combustion using two camera configurations. Also, from the configuration described below, it is possible to visualize the injector spray through the quartz optical jacket from the side view of the head.

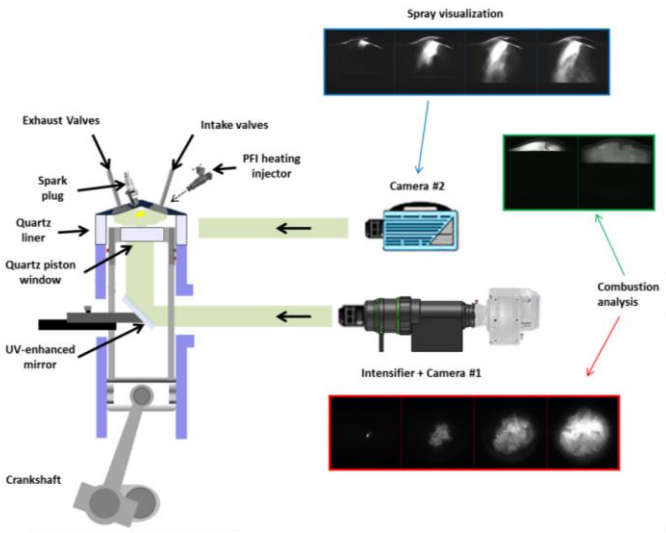

Figure 1 - Experimental arrangement with the cameras configured for the bottom view and side view of the head. Adapted from Merola et al, 2013.

The configuration presented in figure 1 is used for studies of flame propagation by light emission through the quartz piston and consists of a high-speed camera Phanton VEO1310 with a HiCATT 23 S20 100ns intensifier (High-speed Intensified Camera Attachment) from Lambert Instruments. With the camera and intensifier, the optical setup still uses a Nikon UV-Nikkor 105mm f/4.5 lens attached. For all optical measurements, the crank angle encoder signal synchronized the camera and motor through a delay unit (ETU). This configuration has its highest sensitivity in the spectral range between 290 nm and 700 nm, with 50% quantum efficiency at 450 nm. For the full chip configuration (1280×960 pixels) at full resolution, the maximum camera acquisition is 10860 fps; however, to improve the frame rate, we selected 960×960 pixels with a maximum of 13330 fps, allowing us to use 12000 fps, meaning 1 image / CAD at 2000 rpm (1 CAD = 0.083ms). The intensifier increases the camera's sensitivity and allows low-light imaging at frame rates up to 1 MHz (10 MHz burst). It is designed to be operated in conjunction with a camera at up to 300,000 fps, ultimately operating at an aperture width of less than 10 ns (FWHM) with minimal jitter response delay. It also has a software intensifier aperture control where you can control both the gain and the aperture of the intensified image. Furthermore, in the present study, optical access was ensured by a quartz window (64 mm in diameter) fixed in the crown of the elongated piston and a 45° UV mirror in its lower part (see Figure 2). Spatial resolution is 106 μm/pixel and exposure time equivalent to a CAD. The specific configuration of the piston's quartz window allows for 78% coverage of the cylinder bore and 59% of its cross-section.

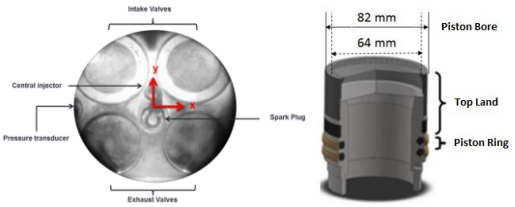

Figure 2 - (Left) Bottom view contrasting intake and exhaust valves, spark plug, pressure transducer and injector. (Right) Dimensions of the optical piston used.

The second camera #2 acquires the lateral images of the quartz cylinder, as seen in Figure 4. A high-speed PCO.dimax S1 (CMOS) camera was used to visualize the penetration of the spray into the cylinder. This configuration has greater sensitivity in the spectral range between 290 nm and 700 nm, with a quantum efficiency of 50% at 450 nm. For the full chip configuration (1008×1008 pixels), the camera's maximum acquisition is 4467 fps; however, to improve the frame rate, 864×896 pixels were selected, allowing for 5400 fps. The setup still uses a Nikon Nikkor 50mm f/1.2D lens attached to the camera. For all optical measurements, the crank angle encoder signal synchronized the camera via a delay unit.

In the present study, only the last 30 cycles are used to process the images and study the propagation of the flames, ensuring that the air/fuel ratio is already stabilized. For image processing, a methodology previously developed in the LCPE was used, detailed in [2] and having as a fundamental concept the work originally developed and [3]. The environment used for processing was the MATLAB platform.

Figure 3 summarizes the steps to perform image processing. Figure 3-a presents the original 8-bit image. The first step is to define a mask that corresponds to the region to be processed, in this case the circular area of the optical piston (Figure 3-b). Next, the contrast and brightness of the image are adjusted to optimize the signal/noise ratio (Figure 3-c), so that it is adequate in terms of identifying the flame front for the application.

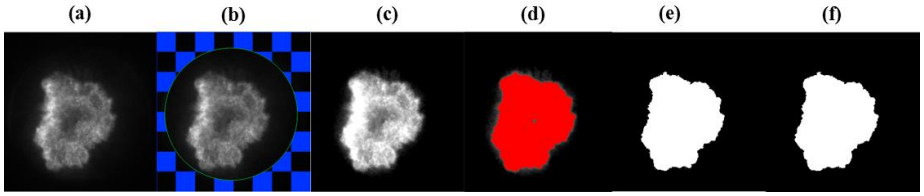

Figure 3 - Script developed for image processing using MATLAB.

For each captured flame image, first the number of pixels within the flame area is calculated and based on the image resolution (in pixels) the area is converted to metric unit. It is observed that the development of the inner surface as a function of the crank angle is directly related to flame propagation. The Waddel Disc Diameter is determined based on the flame area, i.e., it is a diameter of a circular disc containing the same flame area (A) as the previously recorded binary flame.

During engine operation, several factors result in the displacement of the flame front: the burning rate (influenced by chemical kinetics and the pressure/temperature conditions of the environment), diffusion effects, turbulence, swirl and tumble movements, homogeneity of the mixing, heat transfer to the cylinder walls, and expansion of the burnt gases by "pushing" the flame. The individual observation of these effects is a complex task even for optically accessible motors.

However, by expressing all this in a single parameter, the flame propagation speed is important when comparing different combustion situations in the engine. The average flame propagation velocity (Si) is calculated by differentiating the flame radius; therefore, a reverse numerical differentiation scheme was used with WDD during the interval in the intermediate zone of the normalized flame area. The intermediate zone is the period highlighted in figure 4 when there is no interference from the chamber wall and the moment of ignition, therefore the initial and final instants of combustion.

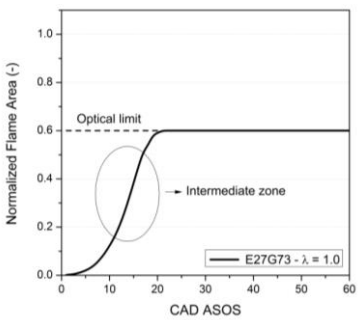

Figure 4 - Middle zone of normalized flame area used to calculate average flame propagation velocity.

3. RESULTS

3.1 Qualitative Analysis of Images

To evaluate the spray injection of the heated or unheated PFI injection system, a series of images of the initial cycles was acquired using the lateral camera. It is important to observe that during these cycles it has not yet been possible to stabilize the IMEP, because despite the continuous supply of the spark, the initial operation of the engine was always surrounded by the absence of misfire or alternation of cycles with some occurrence of combustion.
As it can be seen in figure 5 (a), which shows the injection in the first cycle, the use of the heated injector results in almost immediate fuel vaporization of the fuel, compared to the operation of the system without heating. For this case, it is possible to see a mixture of non-vaporized fuel, which over time condenses into a film on the cylinder wall, while for heated injection the fuel remains vaporized (Figure 5 (b)).

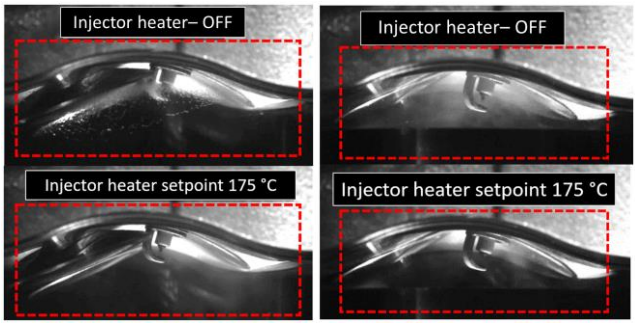

(a) *(b)*

Figure 5 - Spray comparison of unheated injector operation using injector heated to 175°C in the first cycle at (a)1200rpm and (b)2000 rpm with hydrous ethanol; λ=1 and fuel temperature of 10 °C.

Figures 6 to 9 show the visualization of the fuel injection in the 1st, 10th and 20th operation cycles, 1200 and 2000rpm, without injector heating and heated to 175°C, the crankshaft angles 0°CA (PMS), 100°CA (Highest lift/opening of the intake valve) and 140°CA (Closing of the intake valve where the lift is half the maximum opening value). In these tests, the fuel was kept at 10°C in the tank.

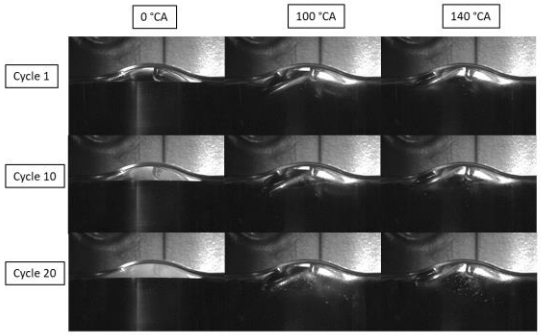

Figure 6 - Side view through the quartz cylinder during fuel injection without injector heating, 1200 rpm, λ = 1 and fuel temperature in the tank 10°C.

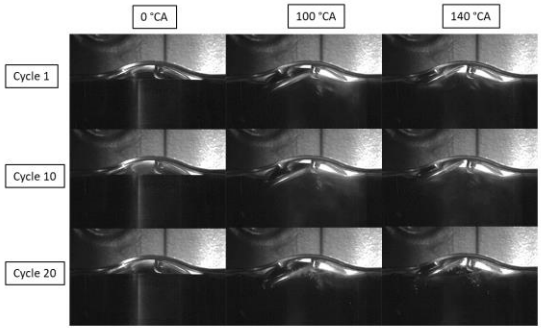

Figure 7 - Side view through the quartz cylinder during fuel injection with heated injector at 175°C, 1200 rpm, λ = 1 and fuel temperature in the tank 10°C.

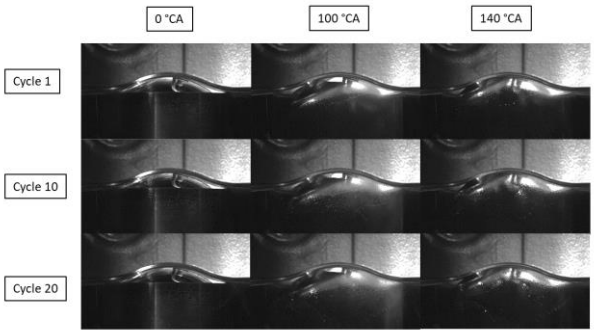

Figure 8 - Side view through the quartz cylinder during fuel injection without injector heating, 2000 rpm, λ = 1 and fuel temperature in the tank 10°C.

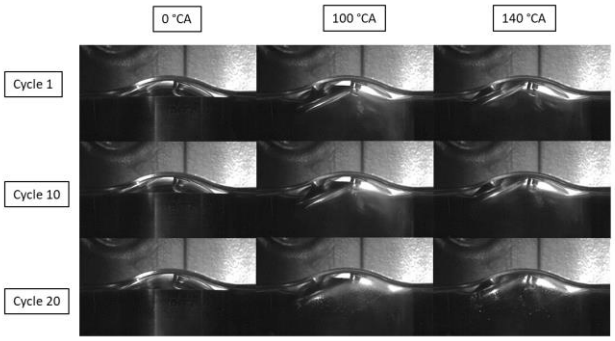

Figure 9 - Side view through the quartz cylinder during fuel injection with injector heated to 175°C, 2000 rpm, λ = 1 and fuel temperature in the tank 10°C.

In general terms, the results presented in Figures 6 to 9 indicate:

1) In a given cycle, especially for the unheated injector, a film of liquid fuel builds up on the cylinder wall as the injection progresses. Without warm-up this occurs pronouncedly from the first cycle. As for the cases with heating, the film of liquid is more pronounced in more advanced cycles, as in the twentieth cycle observed here. This is due to the better vaporization of the fuel by heating it when passing through the injector.

2) As the cycle advances, there is a tendency to increase the accumulated liquid film, especially for the case without heating. However, it is noted that even under the condition of misfire or intermittent combustion, part of the fuel that was in the liquid film is consumed, because qualitatively it is observed that the liquid film at the beginning of the injection of a cycle is relatively smaller than the film present or at the end of the injection of the previous cycles.

Figures 10 to 13 present a sequence of images after the PMS acquired with the combustion of hydrated ethanol for the conditions of 1200 and 2000 rpm, varying the fuel temperature (10 °C and 20°C), in three different conditions for the injector, namely: "T_amb" for condition without injector heating; temperature setpoint at 100°C; and temperature setpoint at 175°C. From the images it can be seen that the luminosity of the flames increases with the heating of the injector. In addition, the flame morphology presents different visual characteristics, showing a greater wrinkling of the flame without the aid of heating and at low rotations. Also, flame propagation appears to be moving more towards the intake valves than the exhaust valves, due to the concentration of fuel in this region during injection, as discussed earlier. Additionally, a tendency of the flame to propagate faster with the increase of the temperature of the injector is noticed, showing that the better vaporization of the fuel improves the formation of the air-fuel mixture inside the cylinder.

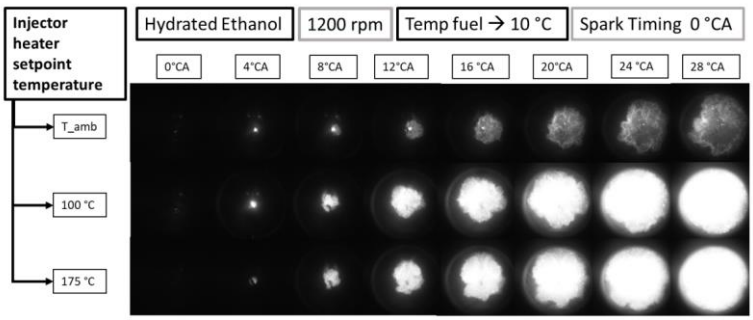

Figure 10 – Front flame development of for different injector heating temperatures and operating conditions: fuel temperature 10°C, at 1200 rpm, λ=1.

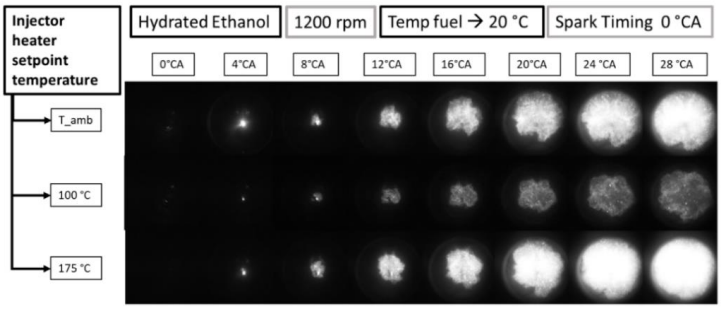

Figure 11 - Development of flame front for different injector heating temperatures and operating conditions: fuel temperature 20°C, at 1200 rpm, λ=1.

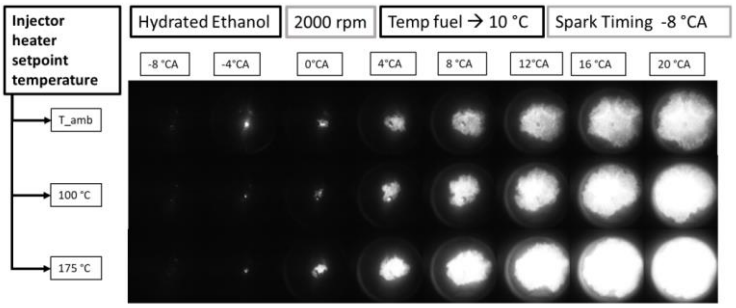

Figure 12 - Development of the flame front of for different injector heating temperatures and operating conditions: fuel temperature 10°C, at 2000 rpm, λ=1.

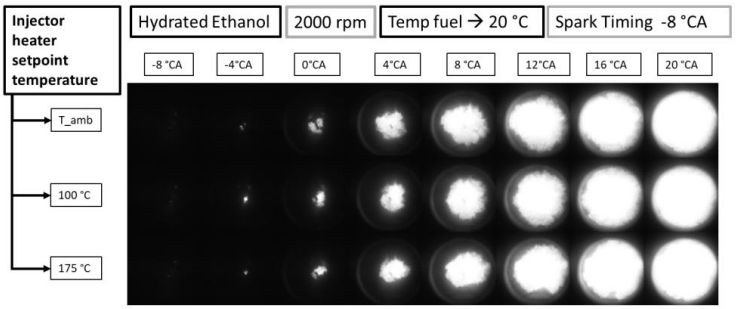

Figure 13 - Development of the flame front of for different injector heating temperatures and operating conditions: fuel temperature 10°C, at 2000 rpm, λ=1.

Figure 14 presents the average flame propagation velocity (VPC) value for different fuel temperatures, injector heating temperature and engine speeds. Results are an average of the last 30 cycles viewed. First, there is a trend of higher VPC for higher rotation. Two points contribute to this; the first is the highest IMEP for 2000 rpm, as will be presented in the next sub-item, that is, there is an increase in pressure and temperature, accelerating combustion; and second is the increase in turbulence with rotation.

Note that for fuel conditioned at 10°C there is a gradual increase in VPC with heating of the injector, which is the expected behavior given the expectation of better vaporization of the fuel. However, this behavior is not replicated in tests with fuel conditioning at 20°C. Note that for 1200rpm there is a drop in the VPC when the injector is heated to 100°C, rising again when it increases to 175°C. For 2000rpm this drop in 100°C is smoother; however, the expectation would be an increase in the VPC.

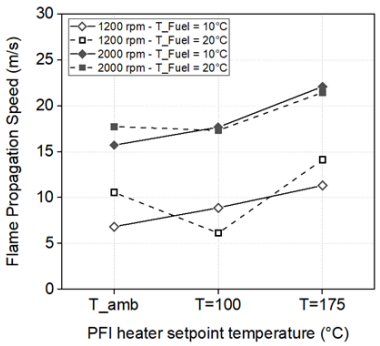

Figure 14 - Flame Propagation Speed for rotations of 1200 and 2000 rpm, fuel temperatures of 10 and 20 °C), with and without heating the injectors.

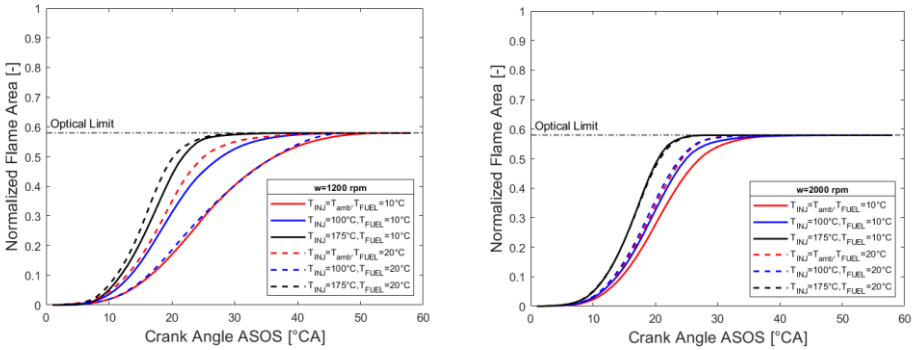

Figure 15 - Normalized flame area at (left) 1200 rpm and (right) 2000 rpm, average of 30 cycles.

3.2 Thermodynamics analysis

Thermodynamic analysis guided the definition of operating points for image acquisition, and the analysis of the last 50 combustion cycles was also used for the parameters shown in Table 3. As a general observation, the results indicate an increase in the IMEP as the temperature increases. The fuel heating rate is high, accompanied by a reduction in its coefficient of variation (CoV_IMEP).

Engine speed [rpm]	Fuel Temperature [°C]	Injector temperature setpoint [°C]	IMEP [bar]	σ_{IMEP} [bar]	CoV_IMEP [%]	AI10 [CAD aTDC]	AI50 [CAD aTDC]
1200	10	T amb	3.84	0.176	4.60	21.57	36.81
		100	4.16	0.136	6.21	18.67	31.70
		175	4.58	0.116	2.92	15.41	25.98
	20	T amb	4.10	0.255	6.21	19.47	32.97
		100	4.05	0.118	2.92	19.73	33.15
		175	4.60	0.104	2.27	15.43	26.12
2000	10	T amb	4.74	0.095	2.16	11.46	24.36
		100	4.78	0.106	2.41	11.11	23.58
		175	4.99	0.060	1.64	9.18	20.66
	20	T amb	4.86	0.103	1.96	10.48	22.80
		100	4.87	0.115	2.18	10.60	22.87
		175	4.95	0.082	1.22	9.39	20.79

Table 3 - Thermodynamic results of the tests performed.

As shown in Figure 16, this trend of increasing IMEP and reducing CoV_IMEP was more pronounced at 1200 rpm, where the late ignition timing (at TDC) generates an initial condition of greater instability.

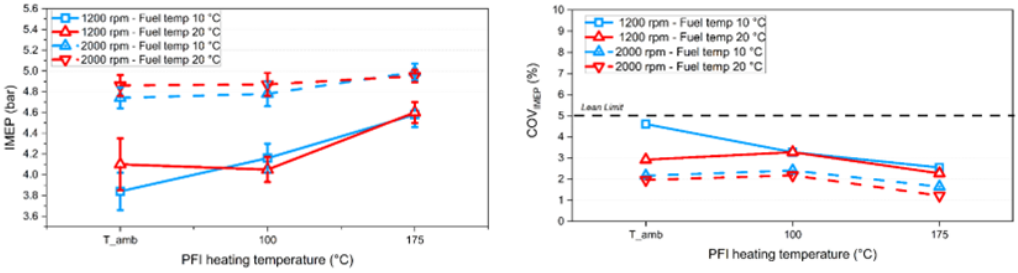

Figure 16 - IMEP (right) and COV_IMEP (left) behavior.

The analysis of the heat released (Figures 17 (a) and (b)) indicates that combustion was anticipated and accelerated for cases with fuel heating and result in higher IMEP and lower CoV_IMEP. Possibly, the increase in the burning rate is a direct consequence of the higher temperature of the gas mixture at the end of compression, given that a relevant part of the fuel evaporation energy was supplied by electrical heating and not by the sensible heat of the charge air.

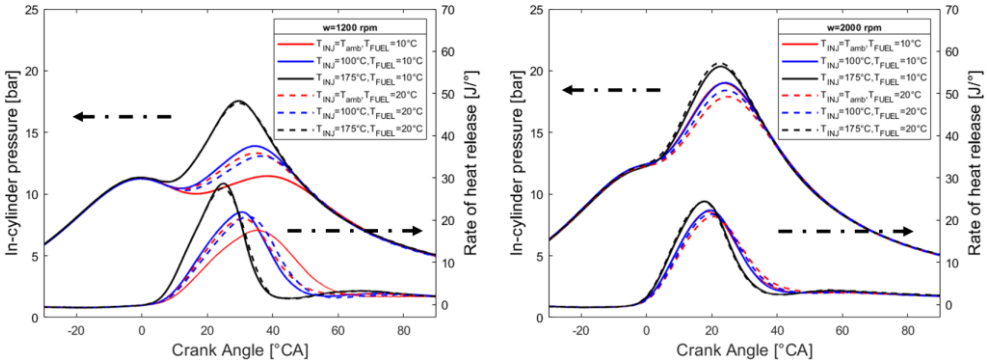

(a) *(b)*

Figure 17 - Cylinder pressure and heat release rate (ROHR) as the injector nozzle is heated to (a) 1200 rpm and (b) 2000rpm.

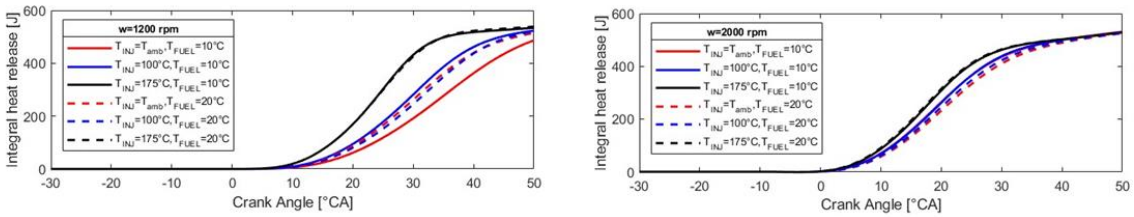

Figure 18 - Heat release during the cycle for both speeds (1200 and 2000 rpm) varying injection and fuel temperature.

As mentioned, the results correspond to the last 50 combustion cycles, with more established trends. Unlike this, the first cycles showed an unstable behavior, as detailed below.

In figures 19 and 20 it can be seen from the average pressure values indicated as a function of the engine operating cycles that the 175°C condition reaches operating stability in approximately 30 cycles, while the others require more than 40 cycles.

For 2000 rpm, this trend is reversed, with the 175°C condition taking 10 to 20 cycles to reach stability, while the others had cycles with practically stabilized combustion within the initial 5 cycles. The hypotheses that could explain this inversion in the behavior of the heated system are not clear; however, it is noted that the higher rotation reduces the instabilities of the initial cycles, and two factors help this behavior: faster engine warm-up and greater turbulence.

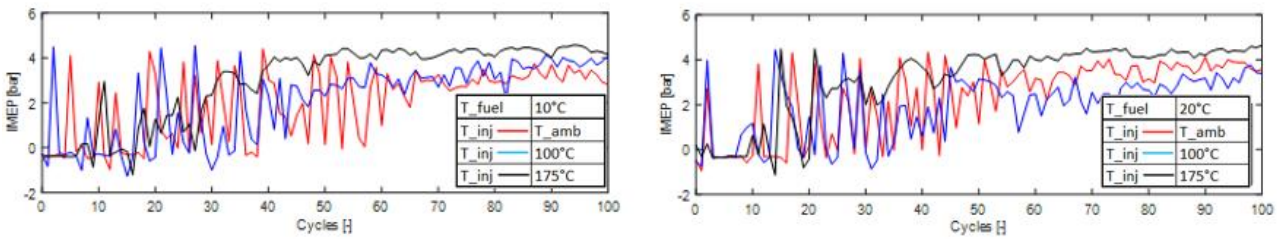

(a) (b)

Figure 19 - IMEP evaluation in the first cycles at 1200 rpm Tfuel (a) 10°C and (b) 20°C.

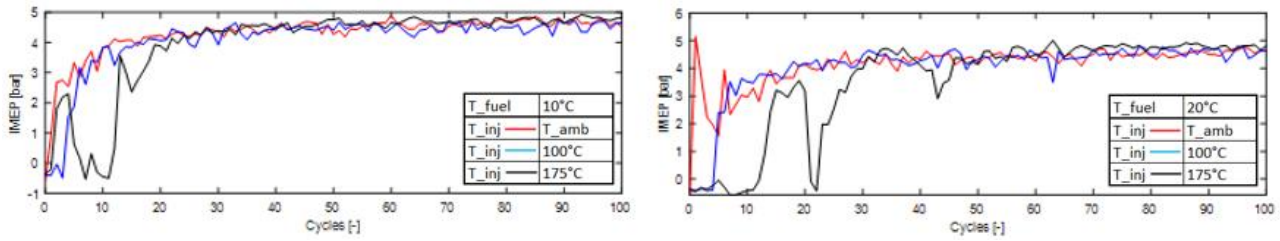

(a) (b)

Figure 20 - IMEP evaluation in the first cycles at 2000 rpm Tfuel (a) 10°C and (b) 20°C.

4. CONCLUSION

It was possible to observe through the lateral images that the fuel enters more vaporized inside the combustion chamber using the heated injector when compared with the operation of the heating system turned off. Thus, when comparing the rotation of 1200 rpm with the rotation of 2000 rpm, it can be observed that larger drops end up b eing produced in greater quantity at low rotations due to smaller influences of the swirl and tumble inside the cylinder. With the use of the heated injector, a smaller recurrence of fuel drops can be noticed because it is more vaporized and smaller amounts of fuel films.

A higher flame propagation speed is observed with increasing injector temperature, showing that temperature improves combustion and improves the air-fuel mixture inside the cylinder. Comparing the curvatures, it was possible to observe an improvement in the operation of ethanol at 10°C at low and high speeds. Because with the injector heated to 175°C, combustion and flame propagation improved, thus improving its stability. This is due to the fuel being injected in a more vaporized state than the operation without the use of the heated injector, leading to a smaller amount of fuel film on the cylinder walls and piston, and due to the increase in the air and fuel temperature, promoting faster combustion.

The results indicate an increase in the IMEP as the fuel heating temperature is increased, accompanied by a reduction in its coefficient of variation (CoV_IMEP). This trend of increasing IMEP and reducing CoV_IMEP was more pronounced at 1200 rpm, where the late ignition timing (at TDC) generates an in itial condition of greater instability. The heat release analysis indicates that combustion was anticipated and accelerated for cases with fuel heating and result in higher IMEP and lower CoV_IMEP. Possibly, the increase in the burning rate is a direct cons equence of the higher temperature of the gas mixture at the end of compression, given that a relevant part of the fuel evaporation energy was supplied by electrical heating and not by the sensible heat of the charge air.

It can be seen from the average pressure values indicated as a function of the engine operating cycles that the 175°C condition reaches operating stability in approximately 30 cycles, while the others require more than 40 cycles. For 2000 rpm, this trend is reversed, with the 175°C condition taking 10 to 20 cycles to reach stability, while the others had cycles with practically stabilized combustion within the initial 5 cycles. It is not clear to the team which hypotheses could explain this reversal in the behavior of the heated system; howe ver, it is noted that the higher rotation reduces the instabilities of the initial cycles, and two factors help this behavior: faster engine warm-up and greater turbulence.

5. REFERENCES

S. S. Merola, G. Valentino, C. Tornatore, e L. Marchitto, “In-cylinder spectroscopic measurements of knocking combustion inaSI engine fuelled with butanol-gasoline blend”, Energy, vol. 62, p. 150–161, 2013, doi: 10.1016/j.energy.2013.05.056.

A. Penaranda, S. D. M. Boggio, P. T. Lacava, S. Merola, e A. Irimescu, “Characterization of flame front propagation during early and late combustion for methane-hydrogen fueling of an optically accessible SI engine”, Int. J. Hydrogen Energy, vol. 43, p. 23538–23557, 2018, doi: 10.1016/j.ijhydene.2018.10.167.

N. Ozdor, M. Dulger, e E. Sher, “Cyclic variability in spark ignition engines a literature survey”, SAE Trans., p. 1514–1552, 1994.

N. Otsu, “A threshold selection method from gray-level histograms”, IEEE Trans. Syst. Man. Cybern., vol. 9, nº 1, p. 62–66, 1979.

J. B. Heywood, Combustion engine fundamentals, nº 1. 1988.

E. R. Malheiro de Oliveira, C. H. Rufino, e P. T. Lacava, “Effects of direct injection and mixture enleament on the combustion of hydrous ethanol and an ethanol-gasoline blend in an optical engine”, Fuel, vol. 327, nº April, p. 125137, 2022, doi: 10.1016/j.fuel.2022.125137.

Colli GB, Castejon D, Salvetti A, Volpato O (2010) Heated Injector Cold Start System for flex-fuel motorcycles. SAE Technical Paper Series. doi: 10.4271/2010-36-0156

6. RESPONSIBILITY NOTICE

The authors are solely responsible for the printed material included in this paper.